

## Single-Residue Alteration in $\alpha$ -Conotoxin PnIA Switches Its nAChR Subtype Selectivity<sup>†</sup>

S. Luo,<sup>‡</sup> T. A. Nguyen,<sup>‡</sup> G. E. Cartier,<sup>‡</sup> B. M. Olivera,<sup>‡</sup> D. Yoshikami,<sup>‡</sup> and J. M. McIntosh<sup>\*,‡,§</sup>

Department of Biology, University of Utah, Salt Lake City, Utah 84112, and  
Department of Psychiatry, University of Utah, Salt Lake City, Utah 84132

Received June 2, 1999; Revised Manuscript Received August 4, 1999

**ABSTRACT:**  $\alpha$ -Conotoxins are disulfide-rich peptides that are competitive antagonists of nicotinic acetylcholine receptors (nAChRs). Despite their small size, different  $\alpha$ -conotoxins are able to discriminate among different subtypes of mammalian nAChRs. In this report, the activity of two peptides from the venom of *Conus pennaceus*,  $\alpha$ -conotoxins PnIA and PnIB, are examined. Although the toxins differ in only two residues, PnIA preferentially blocks  $\alpha 3\beta 2$  nAChRs, whereas PnIB prefers the  $\alpha 7$  subtype. Point mutation chimeras of these  $\alpha$ -conotoxins were synthesized and their activities assessed on *Xenopus* oocytes expressing specific nAChRs. Change of a single residue, Ala10 to Leu, in PnIA (to form PnIA [A10L]) converts the parent peptide from  $\alpha 3\beta 2$ -preferring to  $\alpha 7$ -preferring; furthermore, PnIA [A10L] blocks the  $\alpha 7$  receptor with an IC<sub>50</sub> (12.6 nM) that is lower than that of either parent peptide. Kinetic analysis indicates that differences in affinity among the analogues are primarily due to differences in off-rate, with PnIA [A10L]'s interaction with  $\alpha 7$  having the smallest off-rate ( $k_{\text{off}} = 0.17 \text{ min}^{-1}$ ). Thermodynamic analysis indicates that Leu10 enhances the peptide's interaction with  $\alpha 7$ , but not  $\alpha 3\beta 2$ , receptors, whereas Ser11 (in PnIA [N11S]) reduces its affinity for both  $\alpha 7$  and  $\alpha 3\beta 2$  nAChRs.

Nicotinic acetylcholine receptors are a large and ubiquitously expressed family of ligand-gated ion channels. Peripherally, these receptors mediate rapid synaptic transmission in autonomic ganglia and at the skeletal neuromuscular junction. In the central nervous system, nAChRs<sup>1</sup> may play a further role by modulating neurotransmitter release. Experiments with synaptosomes indicate that distinct subtypes of presynaptic nAChRs can mediate the release of specific neurotransmitters, including dopamine, norepinephrine, glutamate, acetylcholine, GABA, and serotonin (for review see ref 1). To identify which subtype of nAChR is involved in each instance, more ligands with the ability to discriminate among the closely related nAChR subtypes are needed.

$\alpha$ -Conotoxins are a family of small peptides (12–19 amino acids in length) that competitively block nAChRs. Many of these peptides show remarkable selectivity for specific subtypes of nicotinic receptors (2). In general, these peptides can be divided into two groups, those that selectively act on muscle nAChRs, and those that affect neuronal nAChRs (3). The  $\alpha$ -conotoxins studied to date act by binding to the acetylcholine recognition site located at the interface of adjacent  $\alpha$  and non- $\alpha$  subunits of the receptor. That is,  $\alpha$ -conotoxins interact with residues on both the  $\alpha$ - and non- $\alpha$

subunit ( $\delta$ ,  $\gamma$ , and  $\epsilon$  for muscle and  $\beta$  for neuronal) of the nAChR (4–6).

In this report, we focus on two peptides,  $\alpha$ -conotoxins PnIA and PnIB discovered by Fainzilber et al.(7). These peptides were originally described as specific for molluscan nAChRs. In this report, we present detailed results that indicate that they are also active on specific subtypes of rat neuronal nAChRs. The sequences of these conotoxins are almost identical as follows (divergent residues in italics): PnIA, GCCSLPPCAAMNPDYC, and PnIB, GCCSLPPCALSNPDYC. Remarkably, although these peptides differ by only two amino acids, they have distinct receptor selectivities. By use of chimeras of these two peptides constructed by exchanging single residues, we have identified the key determinant that allows them to discriminate between nAChR-subtypes.

### MATERIALS AND METHODS

**Peptide Synthesis. Linear Peptide.** The linear peptides were built on Rink amide resin by Fmoc (*N*-(9-fluorenyl) methoxycarbonyl) procedures with 2-(1H-benzotriole-1-yl)-1,1,3,3-tetramethyluronium tetrafluoroborate coupling, using an ABI model 431A peptide synthesizer. Side chain protection groups of non-Cys residues were in the form of *tert*-butyl (Asp, Ser, Tyr) and trityl (Asn) moieties. Orthogonal protection was used on cysteines, that is, Cys3 and Cys16 were protected as the stable Cys(S-acetamidomethyl), while Cys2 and Cys8 were protected as the acid-labile Cys(S-trityl). After assembly of the resin-bound peptide, the terminal Fmoc group was removed in situ by treatment with 20% piperidine in *N*-methylpyrrolidone. Linear peptide amide was cleaved from resin and purified by RPLC with a 0.1% trifluoroacetic

\* To whom correspondence should be addressed. Department of Biology, University of Utah, 257 South 1400 East, Salt Lake City, UT 84112-0840. Telephone: 801-585-3622. Fax: 801-581-4668. E-mail: mcintosh@bioscience.utah.edu.

<sup>†</sup> This work was supported by NIH grants MH53631 and GM48677.

<sup>‡</sup> Department of Biology.

<sup>§</sup> Department of Psychiatry.

<sup>1</sup> Abbreviations: nAChR, nicotinic acetylcholine receptor; PnIA,  $\alpha$ -conotoxin PnIA.; TFA, trifluoroacetic acid; RPLC, reverse phase liquid chromatography; ACh acetylcholine; DB, dissection buffer, IB, incubation buffer; WB, wash buffer, BSA, bovine serum albumin.

acid/acetonitrile gradient system using previously described methods (8).

**Peptide Cyclization.** To form a disulfide bridge between Cys2 and Cys8 (i.e., the first and third cysteines), the linear peptide fraction obtained by RPLC was dripped (over a period of 2 min) into an equal volume of 20 mM potassium ferricyanide, 0.1 M Tris, pH 7.5. The addition funnel was rinsed with 10 mL of 0.1% TFA, and this rinse was also added to the ferricyanide solution. The solution was allowed to react for a minimum of 30 min with constant stirring at room temperature. The solution was diluted to less than 10% acetonitrile with 0.1% TFA and then vacuum filtered through a disposable C18 extraction cartridge (Alltech #215430). The cartridge was then washed with ~1 L 0.1% TFA to remove the ferricyanide. Peptide was then eluted from the cartridge with ~25 mL of 0.1% TFA and 60% acetonitrile. The monocyclic peptide was then purified by RPLC. Simultaneous removal of the S-acetamidomethyl groups and closure of the second disulfide bridge (Cys3–Cys16, i.e., the second and fourth cysteines) was carried out by iodine oxidation. The monocyclic peptide in RPLC eluent was dripped into an equal volume of a rapidly stirred solution of iodine (10 mM) in H<sub>2</sub>O:TFA:acetonitrile (78:2:20 by volume) over a period of 1 min at room temperature. The reaction was allowed to proceed for another 10 min and terminated by the addition of ascorbic acid sufficient to clear the solution. The solution was diluted 20-fold with 0.1% TFA and the bicyclic peptide purified by RPLC.

**Electrophysiology. RNA Preparation.** cDNA clones encoding nAChR subunits were provided by S. Heinemann and D. Johnson (Salk Institute, San Diego, CA). Neuronal nAChR clones were from rat and muscle nAChR clones were from mouse. cRNA was transcribed using RiboMAX large scale RNA production systems (Promega, Madison, WI). Diguanosine triphosphate (Sigma, St. Louis, MO) was used to synthesize capped cRNA transcripts, according to the manufacturer's protocol. Plasmid constructs of nAChR subunits from mouse ( $\alpha 1$ ,  $\beta 1$ ,  $\gamma$ ,  $\delta$ ) and from rat ( $\alpha 2$ ,  $\alpha 3$ ,  $\alpha 4$ ,  $\alpha 7$ ,  $\beta 2$ ,  $\beta 4$ ) were used as described (9).

**Voltage-Clamp Recording.** Oocytes were harvested and injected with cRNA encoding nAChR subunits as previously described (9). The oocyte recording chamber was constructed of Sylgard and measured 2.5 cm  $\times$  1.5 cm  $\times$  0.4 mm deep (volume 1.5 mL). The chamber was gravity-perfused with either ND96 (96.0 mM NaCl, 2.0 mM KCl, 1.8 mM CaCl<sub>2</sub>, 1.0 mM MgCl<sub>2</sub>, 5 mM HEPES, pH 7.1–7.5) or ND96, containing 1 mM atropine (ND96A) at a rate of ~1.5 mL/min. Solutions were applied to the oocyte through two tubes (2.25 mm o.d.  $\times$  1.75 mm i.d.) positioned ~0.5 mm from opposite poles of the oocyte. All toxin solutions also contained 0.1 mg/mL bovine serum albumin (BSA) to reduce nonspecific adsorption of peptide. The perfusion medium could be switched to one containing peptide or acetylcholine (ACh) by use of a distributor valve (SmartValve, Cavro Scientific Instruments, Sunnyvale, CA) and a series of three-way solenoid valves (model 161T031, Neptune Research, Northboro, MA). All recordings were made at room temperature (~22 °C). ACh-gated currents were obtained with a two-electrode voltage-clamp amplifier (model OC-725B, Warner Instrument Corp., Hamden, CT). Glass microelectrodes, pulled from fiber-filled borosilicate capillaries (1 mm o.d.  $\times$  0.75 mm i.d., WPI Inc., Sarasota, FL) and filled with

3 M KCl, served as voltage and current electrodes. Resistances for voltage and current electrodes were 0.5–3 M $\Omega$  and 0.5–2 M $\Omega$ , respectively. The membrane potential was clamped at –70 mV, and the current signal, recorded through virtual ground, was low-pass filtered (5 Hz cutoff) and digitized at a sampling frequency of 20 Hz. The solenoid perfusion valves were controlled with solid state relays as previously described (8). Data acquisition, measurement of peak responses, and control of the distributor and solenoid valves were automated by a homemade virtual instrument constructed with the graphical programming language LabVIEW (National Instruments, Austin, TX).

To apply a pulse of ACh to the oocyte, the perfusion fluid was switched to one containing ACh for 1 s. This was automatically done at intervals of 1–3 min. The shortest time interval was chosen such that reproducible control responses were obtained with no observable desensitization. This time interval depended upon the nAChR subtype being tested. The concentration of ACh was 1  $\mu$ M for test of  $\alpha 1\beta 1\delta\gamma$ , 1 mM for  $\alpha 7$ , and 300  $\mu$ M for all other nAChRs. The ACh was diluted in ND96A for tests of all except  $\alpha 7$ , in which case the diluent was ND96. For control responses, the ACh pulse was preceded by perfusion with ND96 (for  $\alpha 7$ ) or ND96A (all others). No atropine was used with oocytes expressing  $\alpha 7$ , since it has been demonstrated to be an antagonist of these receptors (10). For responses in toxin (test responses), the perfusion solution was switched to one containing toxin, while maintaining the same interval of ACh pulses. Toxin was continuously perfused until responses reached a steady state. All ACh pulses contained no toxin, for it was assumed that little, if any, bound toxin would have washed away in the brief time (<2 s) it takes for the responses to peak.

**Data Analysis.** The average peak amplitude of three control responses just preceding exposure to toxin was used to normalize the amplitude of each test response to obtain “% response” or “% block”. Each data point of a dose response curve represents the average value  $\pm$  standard error of measurements from at least three oocytes. Dose response curves were fit to the equation: % response = 100/[1 + ([toxin]/IC<sub>50</sub>)<sup>n<sub>H</sub></sup>], where n<sub>H</sub> is the Hill coefficient.

If a receptor has more than one binding site for toxin, then the observed rates of block and unblock of receptor function will not necessarily correspond directly with the rates of receptor-site occupancy. It can be shown (e.g., through equations derived in ref 11) that for receptors with *N* identical toxin-binding sites (where occupation of any one blocks receptor function), if the initial level of receptor-block is about 50% or less, then the observed rate of functional-recovery upon washout of toxin will, to a first approximation, follow a single-exponential time course with a rate constant given by the *k*<sub>off</sub> of toxin-binding. Likewise, if the toxin concentration, [T], is such that the final level of functional-block (i.e., at equilibrium) is about 50% or less, then the observed rate of functional-block is described, to a first approximation, by a single-exponential time course with a rate constant given by {*k*<sub>on</sub>[T] + *k*<sub>off</sub>}, where the kinetics constants are those of toxin-binding. Thus, all kinetic measurements were made under conditions where either the initial or final level of functional-block was about 50% or less. The *k*<sub>on</sub> and *k*<sub>off</sub> values used to determine the *K*<sub>i</sub> values in Table 1 were obtained from single-exponential best-fit curves of experimental data, such as those shown in Figure

Table 1:  $\alpha$ -Conotoxin PnI Activity on  $\alpha 7$  and  $\alpha 3\beta 2$  nAChRs Expressed in *Xenopus* Oocytes

	kinetics of block of $\alpha 7$ nAChRs			IC <sub>50</sub> (nM)/n <sub>H</sub> <sup>a</sup>	
	k <sub>off</sub> (min <sup>-1</sup> ) <sup>b</sup>	k <sub>on</sub> (min <sup>-1</sup> M <sup>-1</sup> ) <sup>b</sup>	K <sub>i</sub> (nM) <sup>c</sup>	$\alpha 7$	$\alpha 3\beta 2$
PnIA[A10L]	0.169	31.5 × 10 <sup>6</sup>	11.1	12.6/1.2	99.3/0.57
PnIB	0.853	13.2 × 10 <sup>6</sup>	84.9	61.3/1.4	1970/0.53
PnIA	1.66	10.5 × 10 <sup>6</sup>	176	252/1.2	9.56/1.0
PnIA[N11S]	6.97	6.17 × 10 <sup>6</sup>	1180	1710/1.6	241/0.61

<sup>a</sup> Determined from dose-response curves of functional block of the receptor (see Figure 2). <sup>b</sup> Calculated by averaging individual experiments ( $n = 3-6$ ) that measured functional block of receptor. <sup>c</sup> Calculated by averaging K<sub>i</sub>s determined in individual experiments (not from k<sub>off</sub>/k<sub>on</sub> values shown in Table). Note, if the nAChR has multiple ligand binding sites, values shown in the table (determined by measurement of receptor function) may differ from values determined by measurement of toxin binding (see Methods).

3; k<sub>off</sub> was obtained directly, and k<sub>on</sub>, from the expression  $k_{obs} = k_{on}[T] + k_{off}$  at a single toxin concentration.

Data fits were performed with Prism software (GraphPad Software Inc., San Diego, CA) running on an Apple Power Macintosh.

**$\alpha$ -Bungarotoxin Binding Assay. Buffers.** The incubation buffer (IB) consisted of (in mM): 10 HEPES, 100 NaCl, and 2 mg/mL BSA, pH adjusted to 7.4 with NaOH. The wash buffer (WB) consisted of IB without BSA. The dissection buffer (DB) consisted of (in mM): 100 K<sub>2</sub>HPO<sub>4</sub>, 2 EDTA, 0.2 PMSF (from a freshly prepared stock of 35 mg/mL PMSF in 95% ethanol), and 0.2% NaN<sub>3</sub> (filtered), with pH adjusted to 7.4 with phosphoric acid. Sucrose-DB (SDB) was DB containing 0.32 M sucrose. Unless otherwise indicated, buffers were used at 4 °C.

**Crude membrane Preparation.** Whole brains, less cerebellum, of male adult Sprague Dawley rats were immersed in DB (10 mL/gm brain). The preparation was homogenized at 2800 rpm with a glass-Teflon homogenizer by six up and down strokes and then centrifuged at 1000g for 10 min. The supernatant was decanted and saved on ice. The pellet was suspended in SDB (5 mL/gm) and centrifuged at 1000g for 10 min. The supernatant was combined with the previous supernatant and centrifuged at 12000g for 30 min. The supernatant was discarded and the pellet was resuspended in DB (5 mL/gm). The preparation was centrifuged at 41000g for 10 min. Supernatant was discarded, and the pellet was resuspended in incubation buffer (2.5 mL/gm). The preparation was mixed in the homogenizer at 650 rpm with 8 up and down strokes. Homogenate was then aliquoted in 1 mL samples and frozen with liquid nitrogen. These membrane preparations were stored at -80 °C until use.

**Binding Assay.** Each sample consisted of 30 mL of crude membrane preparation (approximately 400 mg of protein) diluted with 140 mL of IB. To each sample 10 mL of either IB alone, IB with nicotine (1 mM final concentration), or IB with varying concentrations of  $\alpha$ -conotoxin was added. The mixture was incubated at room temperature (~22 °C) for 30 min. Twenty milliliters of [<sup>125</sup>I]  $\alpha$ -bungarotoxin (500 pM final concentration) was then added, and the mixture was incubated at 37 °C for 30 min. Membranes were subsequently collected on filters with a Brandel cell harvester, and radioactivity on the filters was determined with a gamma

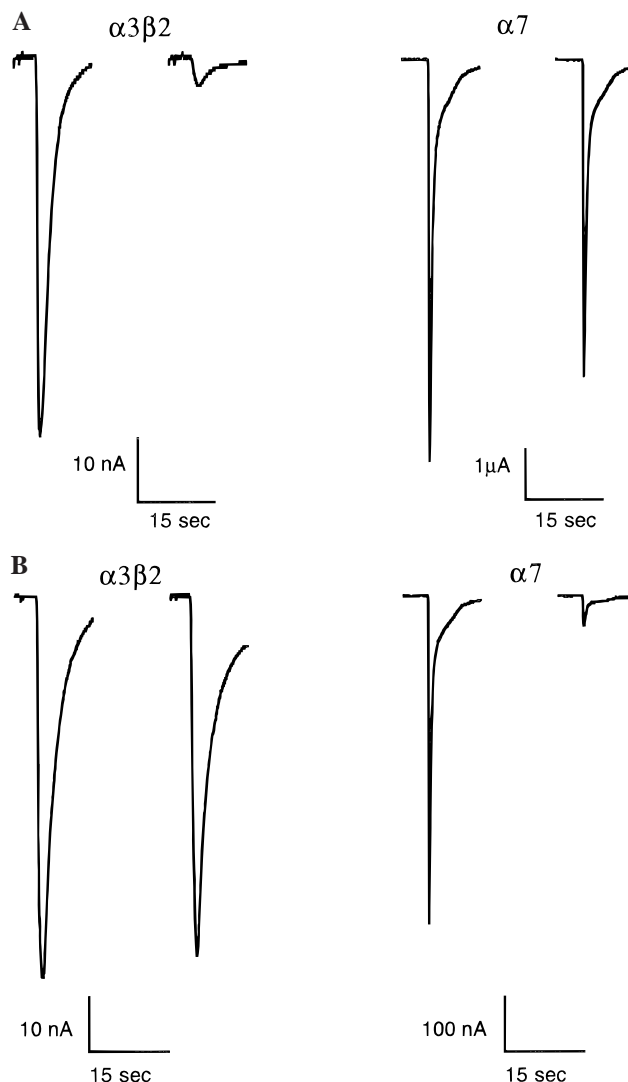


FIGURE 1: PnIA preferentially blocks  $\alpha 3\beta 2$  nAChRs, whereas PnIB preferentially blocks  $\alpha 7$  nAChRs.  $\alpha$ -Conotoxin PnIA (100 nM, Panel A) or PnIB (250 nM, Panel B) was perfusion-applied (see Methods) to oocytes, expressing  $\alpha 3\beta 2$  or  $\alpha 7$  nAChRs. For each pair of traces, control responses are on the left, and responses in the presence of toxin are on the right. PnIA blocked  $92 \pm 1\%$  (mean  $\pm$  S.E.M.) of the ACh response of  $\alpha 3\beta 2$  nAChRs and  $19 \pm 5\%$  of the response of  $\alpha 7$  nAChRs. PnIB blocked  $20 \pm 4\%$  of the ACh response of  $\alpha 3\beta 2$  nAChRs and  $89 \pm 2\%$  of the response of  $\alpha 7$  nAChRs. Experiments were performed 3–7 times and the values averaged. Representative traces are shown in both panels.

counter. The data were analyzed using Prism (Graphpad) software.

## RESULTS

**Activity on Mammalian nAChRs.**  $\alpha$ -Conotoxins PnIA and PnIB were tested on nAChR subunit combinations expressed in *Xenopus* oocytes. Oocytes were perfused with toxin until equilibrium was achieved as measured by the response to brief pulses of ACh applied at 1–3 min intervals.  $\alpha$ -Conotoxins PnIA and PnIB are not only active on mammalian nAChRs, but surprisingly, each has a different subtype preference. The toxins were tested on various subunit combinations including  $\alpha 2\beta 2$ ,  $\alpha 2\beta 4$ ,  $\alpha 3\beta 2$ ,  $\alpha 3\beta 4$ ,  $\alpha 4\beta 2$ ,  $\alpha 4\beta 4$ ,  $\alpha 7$  and  $\alpha 1\beta 1\gamma\delta$ . The two toxins were most active on  $\alpha 3\beta 2$  and  $\alpha 7$  receptors but with opposite preferences (see Figure 1).  $\alpha$ -Conotoxin PnIA preferentially inhibits  $\alpha 3\beta 2$ ,



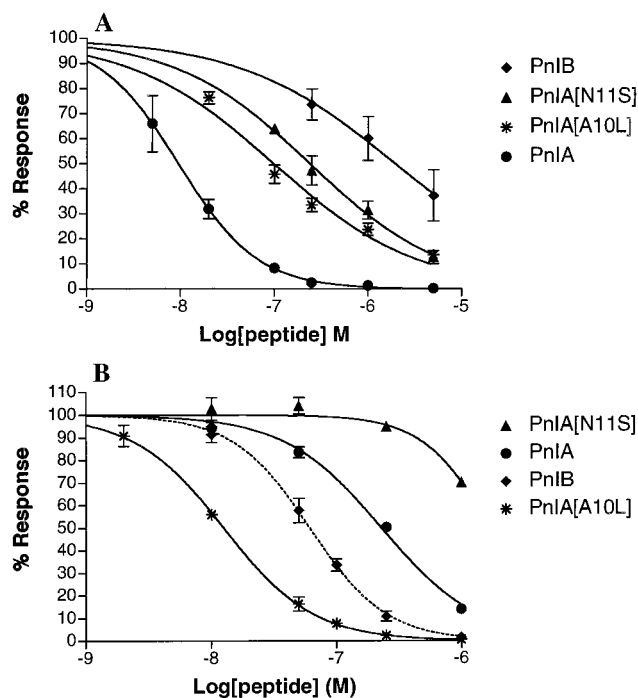


FIGURE 2: Dose-response curves for PnI analogues on nAChR subtypes.  $\alpha$ -Conotoxins were perfusion-applied to oocytes expressing either  $\alpha 3\beta 2$  or  $\alpha 7$  receptors. Response to ACh is plotted as a percentage of the control. Panel A,  $\alpha 3\beta 2$  nAChRs. Panel B,  $\alpha 7$  nAChRs.  $IC_{50}$ s are shown in Table 1. Error bars are S. E. M. and  $n = 3-5$  for each data point.

whereas  $\alpha$ -conotoxin PnIB preferentially inhibits  $\alpha 7$  receptors. This is remarkable, given that the peptides differ by only two amino acids.

**Mutational Analysis of Subtype Preference.** The preferences of these two peptides for different nAChR subtypes provided an intriguing opportunity to investigate structure/function aspects of these peptides. Chimeric analogues were, therefore, constructed; namely, PnIA[A10L] (= PnIB[S11N]) and PnIA[N11S] (= PnIB[L10A]). These two analogues are in effect both chimeras and point mutations of PnIA and PnIB. The oocyte assay was used to compare the potencies of these analogues with those of the naturally occurring peptides (Figure 2). For  $\alpha 3\beta 2$  receptors, as expected  $\alpha$ -conotoxin PnIA is most potent, PnIB is least potent and the two chimeric analogues show intermediate potency. In contrast, for  $\alpha 7$  nAChRs, the chimeras lie outside the potency range of the native peptides.  $\alpha$ -Conotoxin PnIA[N11S] shows only micromolar affinity, whereas the  $\alpha$ -conotoxin PnIA[A10L] analogue shows a low nanomolar  $IC_{50}$ , i.e., its potency exceeds that of either parent peptide. Indeed,  $\alpha$ -conotoxin PnIA[A10L] is the most potent small peptide antagonist reported for  $\alpha 7$  receptors. It should be noted that the Hill coefficients of several of the peptides significantly differ from unity (Table 1). The reasons for this divergence are not clear and require further investigation.

The effect of  $\alpha$ -conotoxin PnIA[A10L] was assessed on other nAChR subtypes as well. At 250 nM PnIA[A10L], the response remaining is (%  $\pm$  S. E. M.):  $\alpha 2\beta 4$ ,  $99 \pm 4$ ;  $\alpha 4\beta 2$ ,  $97 \pm 3$ ;  $\alpha 4\beta 4$ ,  $96 \pm 2$ ;  $\alpha 2\beta 2$ ,  $77 \pm 1$ ; muscle,  $72 \pm 8$ ;  $\alpha 3\beta 4$ ,  $45 \pm 4$ ;  $\alpha 3\beta 2$ ,  $34 \pm 3$ . Data are from three experiments. Although PnIA[A10L] has high potency for the  $\alpha 7$  receptor, it also has considerable activity on other nAChR subtypes, particularly those with an  $\alpha 3$  subunit.

**Kinetic Studies.** The kinetics of the functional block of  $\alpha 7$  receptors was also assessed.  $K_i$ s from individual experiments were determined by dividing  $k_{off}$  by  $k_{on}$ , and these  $K_i$ s from the individual experiments were averaged to obtain the  $K_i$  shown in Table 1. As potency decreases, the off-rates become relatively rapid and are difficult to accurately measure with the present assay procedure (Figure 3). Nevertheless, the  $K_i$ s calculated from the kinetic studies are similar to the  $IC_{50}$ s determined from the dose response studies (see Table 1). The relationship between on- and off-rates is plotted in Figure 3B. The plot indicates that the differences in the  $K_i$ s of the homologues are largely accounted for by differences in off-rates.

**Thermodynamic Analysis.** Taken as a whole, the data suggest that the side-chain of leucine 10 interacts with the  $\alpha 7$  receptor. To quantitate this interaction, the free energy ( $\Delta G$ ) associated with toxin binding to receptor was calculated from  $-RT \ln(K_i)$ , where  $R$  is the gas constant,  $T$  is temperature in K, and  $IC_{50}$  is used as the approximate  $K_i$  (12, 13). By subtracting the  $\Delta G$  of the wild-type toxin (PnIA)-receptor interaction from each mutant toxin-receptor interaction, the difference in free energy of binding mutant vs wild-type peptides ( $\Delta \Delta G$ ) was calculated (see Table 2).  $\Delta \Delta G$  is negative for the N11S mutation for both  $\alpha 3\beta 2$  and  $\alpha 7$  receptors indicating that this mutation unfavorably affects interactions with both receptors. In contrast, for the A10L mutation, the  $\Delta \Delta G$  is negative for  $\alpha 3\beta 2$  receptors but positive for the  $\alpha 7$  subtype, indicating that this single change (Ala to Leu in position 10) is responsible for the switch in affinity of PnIA[A10L] from the  $\alpha 3\beta 2$  to  $\alpha 7$  nAChR subtype. These results strongly suggest direct interaction of the Leu side chain with the  $\alpha 7$  receptor.

**Competition Binding Experiments.** The  $\alpha$ -conotoxin analogues were tested for their abilities to displace the binding of the competitive  $\alpha 7$  antagonist [ $^{125}I$ ]  $\alpha$ -bungarotoxin to rat brain membranes. Results are shown in Figure 4 and indicate that the peptides displace [ $^{125}I$ ]  $\alpha$ -bungarotoxin with the same rank order potency that is seen for block of  $\alpha 7$  homomers expressed in *Xenopus* oocytes. Displacement of  $\alpha$ -bungarotoxin binding is consistent with competitive block of the receptor by the conotoxins.

## DISCUSSION

Crystallography and 2D NMR studies of  $\alpha$ -conotoxins indicate that they share a highly conserved backbone structure (14-18). This backbone appears to serve as a scaffold for the presentation of functional groups. Therefore, differences in receptor affinity and specificity among the  $\alpha$ -conotoxins are likely due to differences in side chain structure. In particular, recently reported crystal structures of  $\alpha$ -conotoxins PnIA and PnIB indicate that their overall structures are highly homologous (Figure 5) (14, 19). One-dimensional NMR analysis of PnIA, PnIB, PnIA[A10L] and PnIA[N11S] indicates that these peptides can exist in more than one conformation, similar to previously reported  $\alpha$ -conotoxins (20) and that the leucine and serine substitutions do not significantly perturb the overall solution structure of the peptide (Scott Beeser and David Goldenberg, personal communication). The residues that differ between the two native peptides (positions 10 and 11) are solvent-exposed and, thereby, may be directly involved in interactions with the nAChRs (see Figure 5).

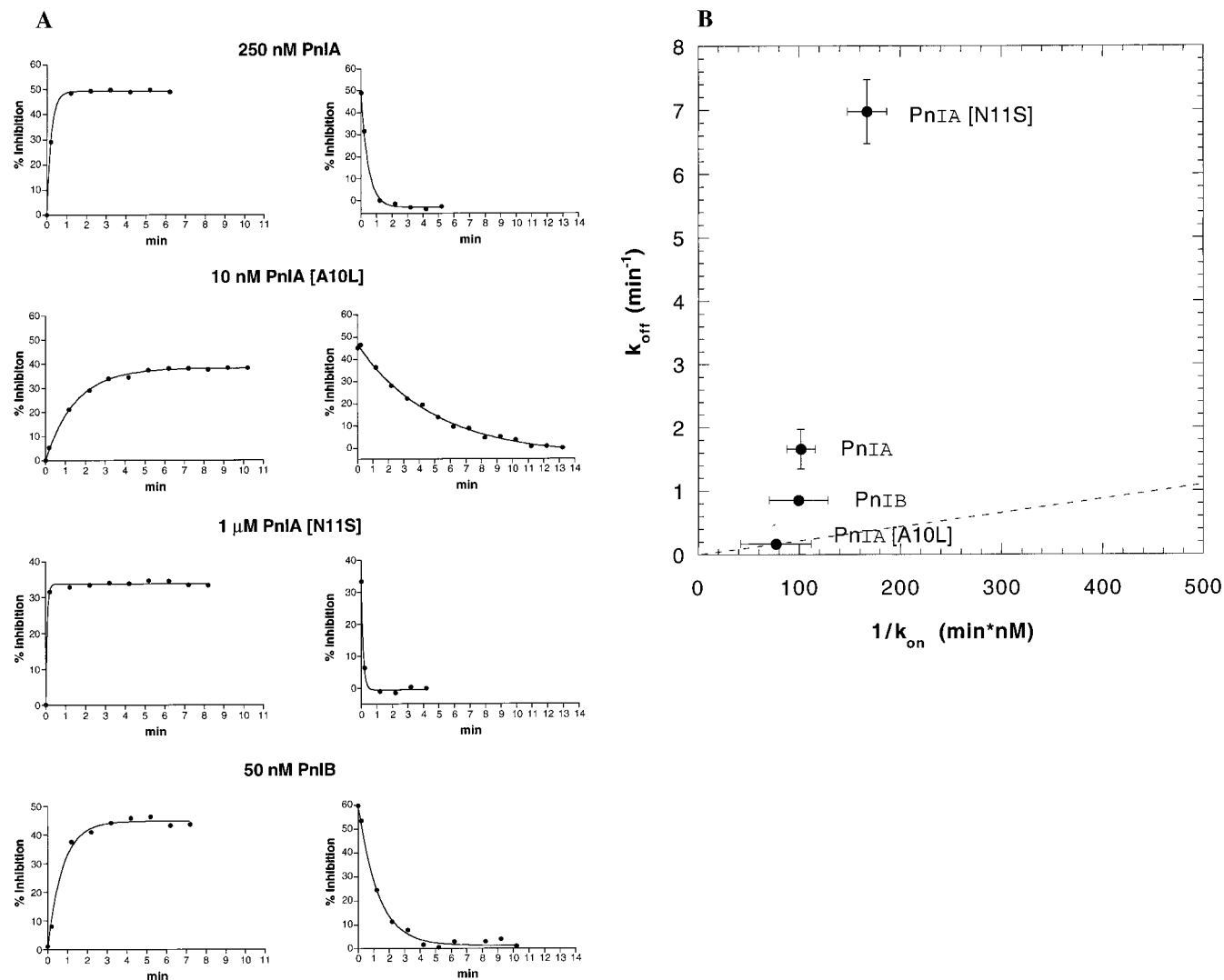


FIGURE 3: Kinetics of PnIA analogues on  $\alpha 7$  nAChRs. Panel A, peak ACh responses during toxin application (left plots) and toxin washout (right) are plotted as a function of time. Responses were fit to a single-exponential function. Representative time courses are shown for each toxin. Experiments were repeated 3–5 times to determine an average value for  $k_{on}$  and  $k_{off}$  from curves such as these. Panel B, mean  $k_{off}$  vs mean  $k_{on}^{-1}$  are plotted. Points nearest the origin have highest affinity. The plot is constructed such that the diagonal dotted line reflects equal changes in  $k_{off}$  and  $k_{on}^{-1}$ . Data show that large differences in  $k_{off}$  are obtained with minimal difference in  $k_{on}^{-1}$ . Error bars are S. E. M.

Table 2: Difference in Free Energy of Binding ( $\Delta\Delta G$ ) for PnIA Mutants

peptide	calculations	$\Delta\Delta G$ (kcal mol $^{-1}$ )	
		$\alpha 7$	$\alpha 3\beta 2$
PnIA[A10L]	( $\Delta G$ PnIA[A10L] – $\Delta G$ PnIA)	1.78	–1.39
PnIA[N11S]	( $\Delta G$ PnIA[N11S] – $\Delta G$ PnIA)	–1.14	–1.91
PnIA[A10L,N11S]	$\Delta\Delta G$ PnIA[A10L] + $\Delta\Delta G$ PnIA[N11S]	0.64 <sup>a</sup>	–3.30 <sup>a</sup>
PnIA[A10L,N11S]	( $\Delta G$ (PnIA[A10L, N11S]) – $\Delta G$ PnIA)	0.84 <sup>b</sup>	–3.16 <sup>b</sup>

<sup>a</sup> Theoretical value if  $\Delta\Delta G$ s are additive. <sup>b</sup> Experimentally determined with PnIB (that is, PnIA[A10L, N11S]).

Although  $\alpha$ -conotoxins PnIA and PnIB were originally reported as mollusc-selective toxins, the results of the present study clearly show that both peptides potently block mammalian nAChRs. Remarkably, the toxins differ in nAChR subtype preference despite having in common fourteen of sixteen amino acids.  $\alpha$ -Conotoxin PnIA preferentially blocks  $\alpha 3\beta 2$  receptors, whereas  $\alpha$ -conotoxin PnIB preferentially

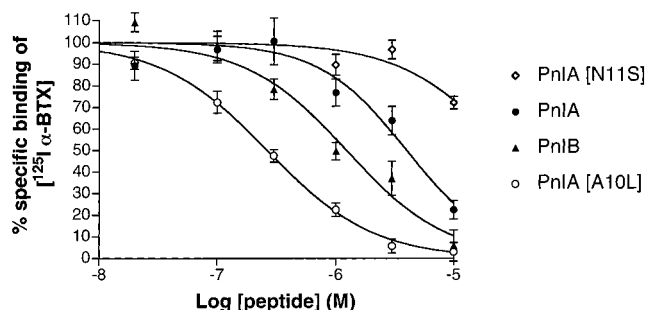


FIGURE 4: Inhibition of  $^{125}I$   $\alpha$ -bungarotoxin binding to rat brain membranes by PnI analogues. The data shown are the mean  $\pm$  S. E. M. ( $n = 3$ ).  $IC_{50}$  (in nM) and  $n_H$ : PnIA[A10L] 0.27, 0.97; PnIB 1.2, 1.0; PnIA 4.0, 1.2; and PnIA[N11S] 27, 1.0.

blocks  $\alpha 7$  homomers. Given that the overall peptide fold is highly conserved, the difference in selectivity must be due to differences in the side chain groups in positions 10 and 11. Both the A10 and N11 residues of PnIA favor binding to the  $\alpha 3\beta 2$  receptor as indicated by the intermediate affinities of the analogues PnIA[A10L] and PnIA[N11S] for

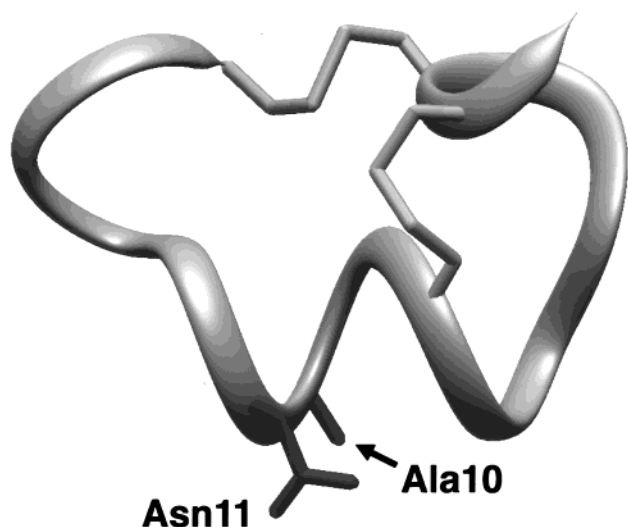
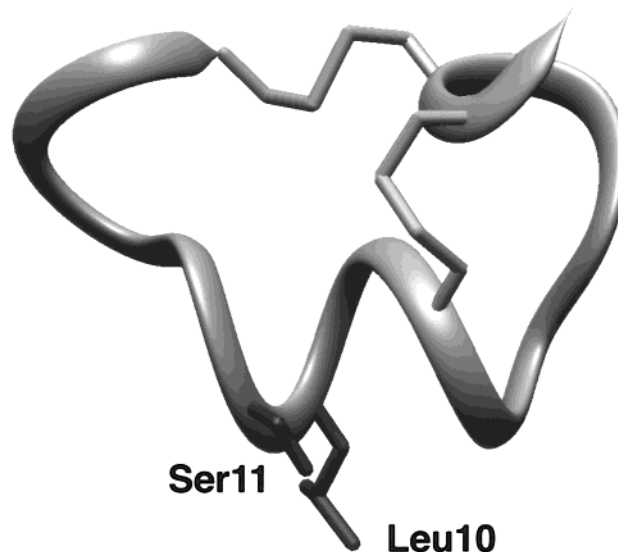
**$\alpha$ -conotoxin PnIA** **$\alpha$ -conotoxin PnIB**

FIGURE 5: Structures of  $\alpha$ -Conotoxins PnIA and PnIB. Peptide backbone is indicated by ribbon structure. Side chains for residues 10 and 11 and disulfide-bonded Cys residues are indicated. The structures were drawn with data reported in refs 14 and 19.

the  $\alpha 3\beta 2$  receptor. However, substitution of leucine for alanine in position 10 of  $\alpha$ -conotoxin PnIA converts the parent peptide from an  $\alpha 3\beta 2$ -preferring ligand to a high affinity  $\alpha 7$ -preferring ligand, with a potency on  $\alpha 7$  receptors exceeding that of either native peptide. In contrast, substitution of serine for asparagine 11 produces a homologue (PnIA-[N11S]) with poorer affinity for  $\alpha 7$  than either native peptide. Kinetic studies indicate that the differences in potencies of these peptides are primarily due to their off-rates.

To examine the interactions of side chains of peptide residues in positions 10 and 11, free energies of the ligand receptor interaction were calculated. For these calculations, the functional  $IC_{50}$  was used to estimate the  $K_d$  of the peptides. Several factors could affect the accuracy of approximating the dissociation constant by measuring functional block of the receptor. However, since  $\Delta\Delta G$  is a ratio, any error in these values cancels in the final equation.

The calculated sums of the  $\Delta\Delta G$ s for the single-mutant peptides on  $\alpha 7$  and  $\alpha 3\beta 2$  receptors approximate the experimentally determined  $\Delta\Delta G$ s for the double-mutant peptide (which is equivalent to the native PnIB) on these nAChR subtypes (see Table 2). This additivity of changes in free energy suggests that the residues in positions 10 and 11 make independent interactions with the receptor. Also, the difference in free energy ( $\Delta\Delta G$ ) for the interaction of mutant peptides with the  $\alpha 7$  and  $\alpha 3\beta 2$  receptors is positive only for the PnIA[A10L]/ $\alpha 7$  receptor pair. This indicates that the Ala to Leu substitution increases the toxin's affinity for the  $\alpha 7$ , but not  $\alpha 3\beta 2$ , receptor. Thus, the leucine side chain appears to make a direct, favorable interaction with residue(s) in the  $\alpha 7$  receptor (possibly a hydrophobic pocket). In contrast, the Asn to Ser substitution decreases the peptide's affinity for both receptor subtypes. This suggests that the Asn side chain makes favorable contacts with residue(s) in both the  $\alpha 3\beta 2$  and  $\alpha 7$  receptors. These residues may be entirely conserved between  $\alpha 3\beta 2$  and  $\alpha 7$  nAChR subtypes,

though the difference in magnitude of change in affinity after the Asn to Ser substitution suggests that some receptor residues at this site are different.

The  $\alpha$ -conotoxin analogues were also investigated with respect to their affinities for native nAChRs by measuring their ability to displace [ $^{125}I$ ]  $\alpha$ -bungarotoxin binding to rat brain membranes. The results indicate that the peptides do in fact displace this  $\alpha 7$ -selective ligand. The  $IC_{50}$ s reported from these binding experiments are higher than those seen in the oocyte experiments where receptor function is assayed. There are several possible explanations for this. First, nicotinic receptors are pentamers, and, therefore, in the case of  $\alpha 7$  homomers (as expressed in *Xenopus* oocytes) there are five possible binding sites for acetylcholine and competitive antagonists. If a receptor has  $N$  identical and independent binding sites for an antagonist, and occupation of any one (or more) of these sites by antagonist is sufficient to block receptor function, then the relationship between the  $IC_{50}$  (as determined by block of receptor function) and  $K_d$  (toxin binding) is given by

$$\frac{IC_{50}}{K_d} = \sqrt[N]{2} - 1$$

Thus, for  $N = 5$ ,  $IC_{50}/K_d = 0.15$ .

There is also a difference in the reported  $IC_{50}$  and  $K_d$  values for the  $\alpha 7$ -selective ligand methyllycaconitine. The  $IC_{50}$  (as determined by functional block of chick  $\alpha 7$  receptor expressed in oocyte) is 0.025 nM (21), whereas the  $K_d$  (as determined by competition binding assays using  $^{125}I$   $\alpha$ -bungarotoxin to chick ciliary ganglion) is 2.8 nM (22). In neonatal rat, methyllycaconitine blocks the response of hippocampal neurons to ACh with an  $IC_{50}$  of  $\sim 200$  pM, whereas methyllycaconitine has a  $K_d$  of  $\sim 4$  nM for inhibiting  $^{125}I$   $\alpha$ -bungarotoxin binding to (adult) rat hippocampus (23).

Additional factors, however, must play a role in the difference between  $IC_{50}$  and  $K_d$  given the magnitude of the discrepancies. Structural differences between receptors expressed in oocytes and native receptors also could account for the observed differences between  $IC_{50}$  and  $K_d$ . For example, differences in posttranslational modification or subunit assembly or the presence of non- $\alpha 7$  subunits in native receptors.

However, the rank order of potency for the peptides in blocking the  $\alpha 7$  homomer function in *Xenopus* oocytes is the same as that in blocking  $\alpha$ -bungarotoxin binding to  $\alpha 7$  receptors in rat brain. This suggests that, at least to a first approximation,  $\alpha 7$  homomers expressed in oocytes are comparable to the native  $\alpha$ -bungarotoxin-binding receptors in brain, and that the PnI series of  $\alpha$ -conotoxin ligands will be useful to study native  $\alpha 7$ -bearing receptors.

Nicotinic receptors are implicated in a number of biological processes as well as pathological disorders. Given the numerous subtypes of receptors present in vivo, the availability of subtype-selective ligands is important. In the present study, we have demonstrated that the addition of a hydrophobic side chain to the common structural scaffold of the  $\alpha$ -conotoxins is sufficient to switch its specificity from one nAChR subtype to another. This lends hope to the notion that the conserved  $\alpha$ -conotoxin structural scaffold can be exploited to lead to the synthesis other new ligands with novel selectivities.

## REFERENCES

1. Wonnacott, S. (1997) *Trends Neurosci.* 20, 92–98.
2. McIntosh, J. M., Olivera, B. M., and Cruz, L. J. (1998) *Methods Enzymol.* 294, 605–624.
3. McIntosh, J. M., Santos, A. D., and Olivera, B. M. (1999) *Annu. Rev. Biochem.*, in press.
4. Sine, S. M., Kreienkamp, H.-J., Bren, N., Maeda, R., and Taylor, P. (1995) *Neuron* 15, 205–211.
5. Sugiyama, N., Marchot, P., Kawanishi, C., Osaka, H., Molles, B., Sine, S. M., and Taylor, P. (1998) *Mol. Pharmacol.* 53, 787–794.
6. Harvey, S. C., McIntosh, J. M., Cartier, G. E., Maddox, F. N., and Luetje, C. W. (1997) *Mol. Pharmacol.* 51, 336–342.
7. Fainzilber, M., Hasson, A., Oren, R., Burlingame, A. L., Gordon, D., Spira, M. E., and Zlotkin, E. (1994) *Biochemistry* 33, 9523–9529.
8. Luo, S., Kulak, J. M., Cartier, G. E., Jacobsen, R. B., Yoshikami, D., Olivera, B. M., and McIntosh, J. M. (1998) *J. Neurosci.* 18, 8571–8579.
9. Cartier, G. E., Yoshikami, D., Gray, W. R., Luo, S., Olivera, B. M., and McIntosh, J. M. (1996) *J. Biol. Chem.* 271, 7522–7528.
10. Gerzanich, V., Anand, R., and Lindstrom, J. (1994) *Mol. Pharmacol.* 45, 212–220.
11. Jacobsen, R., Yoshikami, D., Ellison, M., Martinez, J., Gray, W. R., Cartier, G. E., Shon, K., Groebe, D. R., Abramson, S. N., Olivera, B. M., and McIntosh, J. M. (1997) *J. Biol. Chem.* 36, 22531–22537.
12. Schreiber, G., and Fersht, A. R. (1995) *J. Mol. Biol.* 248, 487–486.
13. Goldstein, S. A. N., Pheasant, D. J., and Miller, C. (1994) *Neuron* 12, 1377–1388.
14. Hu, S.-H., Gehrmann, J., Guddat, L. W., Alewood, P. F., Craik, D. J., and Martin, J. L. (1996) *Structure* 4, 417–423.
15. Shon, K., Koerber, S. C., Rivier, J. E., Olivera, B. M., and McIntosh, J. M. (1997) *Biochemistry* 36, 15693–15700.
16. Gehrmann, J., Alewood, P. F., and Craik, D. J. (1998) *J. Mol. Biol.* 278, 401–415.
17. Hill, J. M., Oomen, C. J., Miranda, L. P., Bingham, J.-P., Alewood, P. F., and Craik, D. J. (1998) *Biochemistry* 37, 15621–15630.
18. Hu, S.-H., Loughnan, M., Miller, R., Weeks, C. M., Blessing, R. H., Alewood, P. F., Lewis, R. J., and Martin, J. L. (1998) *Biochemistry* 37, 11425–11433.
19. Hu, S.-H., Gehrmann, J., Alewood, P. F., Craik, D. J., and Martin, J. L. (1997) *Biochemistry* 36, 11323–11330.
20. Favrau, P., Krimm, I., Le Gall, F., Bobenrieth, M. J., Lamthanh, H., Bouet, F., Servent, D., Molgo, J., Menez, A., Letourneux, Y., and Lancelin, J. M. (1999) *Biochemistry* 38, 6317–6326.
21. Palma, E., Bertrand, S., Binzoni, T., and Bertrand, D. (1996) *J. Physiol. (London)* 491, 151–161.
22. Vijayaraghavan, S., Pugh, P. C., Zhang, Z. W., Rathouz, M. M., and Berg, D. K. (1992) *Neuron* 8, 353–362.
23. Manickavasagam, A., Pereira, E. F. R., Wonnacott, S., and Albuquerque, E. X. (1992) *Mol. Pharmacol.* 41, 802–808.

BI991252J